Journal of Materials Chemistry A

Accepted Manuscript

This article can be cited before page numbers have been issued, to do this please use: N. Kurra, R. Wang and H. N. Alshareef, *J. Mater. Chem. A*, 2015, DOI: 10.1039/C5TA00829H.

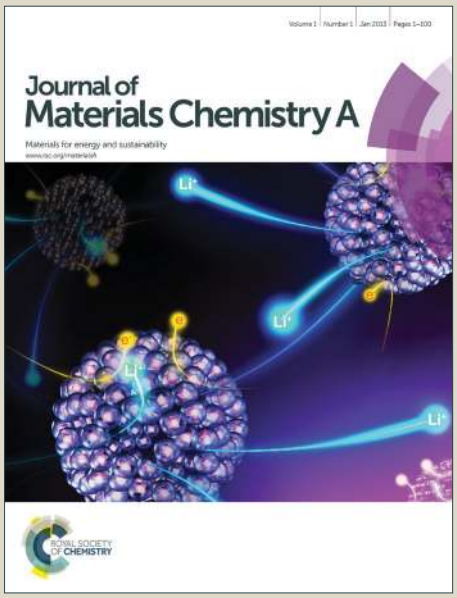

ROYAL SOCIETY OF CHEMISTRY

www.rsc.org/materialsA

View Article Online
DOI: 10.1039/C5TA00829H

Table of Content (ToC)

All-conducting polymer electrodes for asymmetric supercapacitors

Solid state asymmetric supercapacitors are fabricated employing the conducting polymers such as polyaniline and poly(3,4-ethylenedioxythiophene) as positive and negative electrodes, respectively.

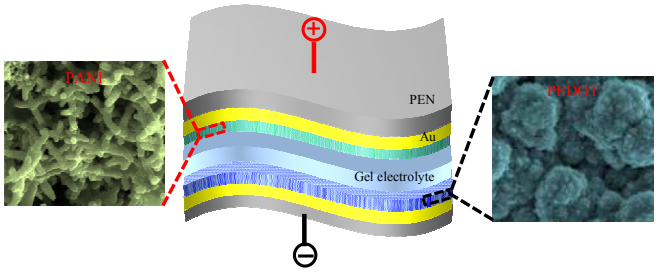

DOI: 10.1039/C5TA00829H

Cite this: DOI: 10.1039/c0xx00000x

www.rsc.org/xxxxxx

ARTICLE TYPE

All Conducting Polymer Electrodes for Asymmetric Solid-State Supercapacitors

Narendra Kurra, Ruiqi Wang, and H. N. Alshareef*

Received (in XXX, XXX) Xth XXXXXXXXX 20XX, Accepted Xth XXXXXXXXX 20XX

DOI: 10.1039/b000000x

In this study, we report the fabrication of solid-state asymmetric supercapacitors (ASCs) based on conducting polymer electrodes on a plastic substrate. Nanostructured conducting polymers of poly(3,4-ethylenedioxythiophene), PEDOT, and polyaniline (PANI) are deposited electrochemically over Au-coated polyethylene naphthalate (PEN) plastic substrates. Due to electron donating nature of oxygen groups in the PEDOT, reduction potentials are higher, allowing it to use as a negative electrode material. In addition, high stability of PEDOT in its oxidised state, makes it capable to exhibit electrochemical activity in a wide potential window. This can qualify PEDOT to be used as a negative electrode in fabricating asymmetric solid state supercapacitors with PANI as positive electrode while employing polyvinylalcohol (PVA)/H_2SO_4 gel electrolyte. The ASCs exhibit a maximum power density of 2.8 W/cm^3 at an energy density of 9 mWh/cm^3, which is superior to the carbonaceous and metal oxide based ASC solid state devices. Furthermore, the tandem configuration of asymmetric supercapacitors is shown to be capable of powering a red light emitting diode for about 1 minute after charging for 10 seconds.

Introduction

Flexible electronic devices are in the necessity for the development of light-weight and solid state energy storage units on the flexible platforms such as plastic substrates.[1-3] Supercapacitors, also called electrochemical capacitors have become potential energy storage units due to their higher energy density compared to conventional electrostatic capacitors, and higher power density compared to batteries along with the fast charge-discharge rates and long cycle life.[3-7]

Carbonaceous materials with tunable surface area in different morphologies have been employed as electrodes for electrochemical double layer capacitors (EDLCs).[8-11] Since the charge is stored through the formation of electrochemical double layers, capacitance values are typically lower for these carbonaceous materials compared to the pseudocapacitors which involve Faradaic reactions for storing the charge.[2,8,12] In this context, several pseudo-capacitive materials such as transition metal oxides/hydroxides[12,13] and conducting polymers[2,3,14] have been employed to enhance the capacitance values due to their fast surface redox reactions. Besides the capacitance, the energy density ($E = ½ C * V^2$) of a supercapacitor is determined by the square of the operating potential window of the electrolyte.[6] Hence, non-aqueous electrolytes (organic and ionic liquids) are preferred due to their wide electrochemical potential windows (3-4 V) over the aqueous electrolytes (1 V) in obtaining superior energy density values. However; non-aqueous electrolytes suffer from poor ionic conductivity, flammability and high cost.[15] Thus, there is an urge to extend the electrochemical potential window of aqueous electrolytes beyond 1 V by embracing the asymmetric design of electrode materials.[15-18]

Mostly, carbonaceous materials have been employed as negative electrode materials while metal oxides/hydroxides and conducting polymers were used as positive electrode materials in designing asymmetric supercapacitors (ASCs) employing liquid and solid electrolytes.[15-20] Despite of the higher potential window of asymmetric supercapacitor, the cell capacitance, C_T, is limited by the lower capacitance electrode, mostly the capacitance of the negative carbonaceous electrode material, C_-, ($1/C_T = 1/C_+ + 1/C_-$).[16-21] In order to boost up the cell capacitance of the ASC, metal oxides such as Fe_2O_3, V_2O_5 have been employed as negative electrode materials which exhibit reversible redox reactions.[22-25] However, the poor conducting nature of these oxides would result in the lower values of power density and they should be synthesized in the form of composites with the carbonaceous materials for the better performance.[15]

Conducting polymers (CPs) have become attractive candidate materials for supercapacitors due to their many salient characteristics such as high electrical conductivity, ease of solution processing, low cost, electrochemical stability and reversibility between redox states through doping/dedoping processes.[26-29] Conducting polymer supercapacitors have been broadly classified into three categories such as Type I symmetric supercapacitors using p-dopable CPs, Type II asymmetric with two different p-dopable CPs and type III symmetric SC which can be both p and n-doped. CPs can be easily deposited over the current collectors either by chemical or electrochemical methods in a binder-free manner.[26-30] Recently, conducting polymers such as polyaniline, polypyrrole and PEDOT have been employed in combination with carbonaceous materials and metal oxides (MnO_2, MoO_3, V_2O_5) in designing the asymmetric

View Article Online
DOI: 10.1039/C5TA00829H

supercapacitors.[21,31-35] In this study, we investigate the electrochemical performance of an asymmetric supercapacitor made out of two conducting polymers employing gel electrolyte.

Here, we employ a simple single-step electrodeposition method to fabricate all-conducting polymer based ASC without employing carbonaceous material. Specifically, we have used conducting polymer, poly(3,4-ethylenedioxythiophene) (PEDOT), due to its electrochemical activity in a wide potential window (1.4 V), as the negative electrode material. Simultaneously, Polyaniline (PANI) was used as a positive electrode material to fabricate asymmetric solid-state supercapacitors on Au-coated plastic PEN substrates while employing PVA/H_2SO_4 gel electrolyte, a maximum energy density of 12 mWh/cm^3 was achieved. These values are superior to asymmetric solid-sate supercapacitors based on MnO_2 Nanowires//Fe_2O_3 Nanotubes electrodes (E = 0.55 mWh/cm^3) and solid-state symmetric supercapacitors based on conducting polymer (ppy, E = 1 mWh/cm^3; PANI/pencil/paper, E = 0.32 mWh/cm^3) electrodes. Furthermore, the tandem configuration of our asymmetric supercapacitors is used to glow a red light emitting diode.

Results and discussion

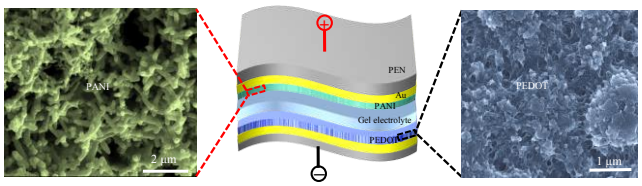

Fig. 1 Schematic illustration of fabrication of asymmetric supercapacitors based on conducting polymer electrodes. PANI//PEDOT ASC device with aqueous gel electrolyte. SEM micrographs of PANI nanofibers and nanostructured PEDOT (false colored). Thickness of the each layer, PEN, 125 μm; Au, 150 nm; PANI, 2.5 μm; gel electrolyte, 60 μm; PEDOT, 4.5 μm.

The schematic shown in Fig.1 illustrates the fabrication of ASC based on all-conducting polymer electrodes over the plastic PEN sheet as a supporting platform. Since PEN is insulating, a conductive coating was formed by depositing Au metal film through thermal evaporation. Au/PEN was used as a conducting platform for the electrochemical deposition of conducting polymers such as PEDOT and PANI from their monomer solutions of EDOT and aniline with sulphuric acid as supporting electrolyte, respectively. These PEDOT/Au/PEN and PANI/Au/PEN were employed as negative and positive electrodes, respectively (see Fig. 1) in fabricating conducting polymer based asymmetric solid state supercapacitor employing aqueous gel electrolyte. PANI nanofibers were grown over Au/PEN substrate through galvanostatic electrodeposition. Nanostructured PEDOT was grown on Au/PEN sheet via electrodepoistion under potentiostatic conditions as shown in SEM micrograph in Fig. 1.

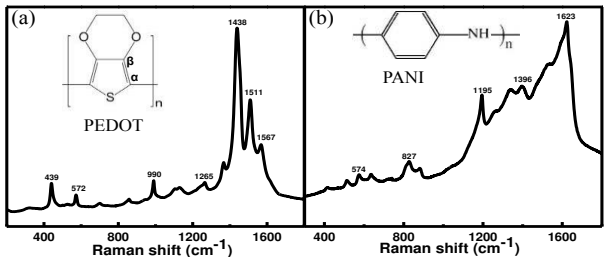

Fig. 2 (a) and (b) Raman spectra of electrochemically deposited PEDOT and PANI from their corresponding monomer aqueous solutions, respectively.

The chemical composition and bonding of PEDOT and PANI grown over Au/PEN were characterized by Raman spectroscopy and the spectra are shown in Figs. 2a and 2b. As shown in Fig. 2a, several characteristic peaks of PEDOT can be seen in the Raman spectrum and the assignment is as follows. The most intense peak at 1440 cm^{-1} corresponding to symmetric stretching of C_α=C_β which can also provide information about the extent of oxidation level.[36] While the asymmetric stretching of C_α = C_β results in the bands at 1570 and1509 cm^{-1}. The peak at 1367 cm^{-1} corresponds to C_β–C_β inter-ring stretching and at 1264 cm^{-1} represents C_α – C_α inter-ring stretching. The peak at 1105 cm^{-1} represents C-O-C deformation, 988 cm^{-1} represents C-C anti-symmetrical stretching mode, 702 cm^{-1} corresponds to symmetric C-S-C deformation, 573 cm^{-1} due to oxy-ethylene ring deformation and 440 cm^{-1} correspond to SO_2 bending, confirms the doping of sulfate and bisulfate anions (from sulphuric acid) in PEDOT nanostructures during the electrochemical deposition.[37] In the case of PANI/Au/PEN, the bands at 1623 and 1529 cm^{-1} correspond to C=C and C=N stretching vibrations, bands at 827 and 415 correspond to C-H deformation while bands at 1396, 1340, 1262, 1195, 741, 574 and 514 cm^{-1} are related to benzene ring deformations (see Fig. 2b).[38]

PEDOT exhibits lower specific capacitance when compared to other conducting polymers (PANI, Ppy) due to larger molecular weight of the monomer unit and also low doping level.[39] However, PEDOT is an electroactive with high capacitance over a wide potential window (1.4 V), in principle, can be employed as a positive and also negative electrode material in energy storage devices (see Electronic Supplementary Information, ESI, Fig. S1). PEDOT in its oxidized form is highly conducting and environmentally stable and hence p-doped PEDOT has been explored as a positive electrode material in most of the previous reports.[2,27,29] Conducting polymer supercapacitors have been broadly classified into three categories such as Type I symmetric supercapacitors using p-dopable conducting polymers (CPs), Type II asymmetric with two different p-dopable CPs, and type III symmetric supercapacitors which can be both p and n-doped.[1] As n-doped (de-doped) CPs is less conducting and more unstable, limiting the usage of CPs as an anode material.[1,2] PEDOT has been a promising electrode material for Type I and asymmetric type II supercapacitors because of its high stability in the oxidation state.[40,41] However, it has been demonstrated that various doped states of PEDOT can be used as cathode and anode for making rechargeable batteries.[42,43] Recently, it was demonstrated that improving the conductivity of PEDOT:PSS by

View Article Online
DOI: 10.1039/C5TA00829H

solvent annealing can induce electrochemical activity in a wider potential window by shifting reduction potential towards more negative values.[44] J. Ahonen et al. have performed p- and n-doping of PEDOT in anhydrous organic medium and observed that PEDOT gets n-doped beyond a potential of -1 V.[45] Further, they found that the reduced form of PEDOT is not stable even in an extremely dry oxygen-free environment, which may severely hampers the use of PEDOT in the extreme negative potential windows.[45] However, in our case we have observed that PEDOT is quite stable until the potential of -0.5 V. Beyond the potential of -0.5 V, we have observed a sudden rise in the negative current which can be attributed to the hydrogen evolution reaction as the electrolyte medium is 1M H_2SO_4 (see Fig. S1a, ESI). Hence, the conductivity, higher degree of polymerization and electron donating nature of alkoxy moieties of PEDOT, make it usable as an anode material by shifting the reduction potentials towards higher negative potentials, without getting it into the n-doped state.[44,45]

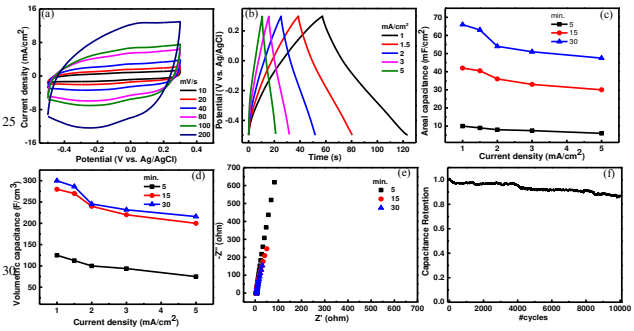

Fig. 3 Electrochemical behavior of PEDOT/Au/PEN electrode in 3-electrode configuration in the negative potential window. (a) Cyclic voltammograms (CVs) and (b) galvanostatic charge-discharge (CD) curves for PEDOT (30 min.)/Au/PEN electrode in the negative potential window. (c) and (d) Areal and volumetric capacitance of PEDOT deposited for different times vs. current density. (e) Nyquist plots of various PEDOT/Au/PEN electrodes. (d) Electrochemical stability of the PEDOT/Au/PEN electrode over 10000 cycles at a current density of 2 mA/cm^2.

We have investigated the electrochemical behavior of PEDOT/Au/PEN electrode in the negative potential window (0.3 to -0.5 V) in 1M H_2SO_4 electrolyte in 3-electrode configuration. As shown in Fig. 3a, the CV curves are seen as rectangular in shape with the appearance of broad redox peaks, due to electrochemical doping of PEDOT by the electrolyte ions. However, it is difficult to assign the oxidation/reduction (doping/dedoping) due to short-life times of intermediate unstable species. Chen et al., have performed fast scan cyclic voltammetry at low temperature to understand the electrochemical behavior of PEDOT.[46] PEDOT is quite stable until the potential of -0.5 V due to its doped state which may get de-doped below -0.5 V resulting in loss of capacitance due to diminished conductivity.[47,48] The charge-discharge curves are seen as linear in the potential window of 0.3 to -0.5 V at different current densities from 1 to 5 mA/cm^2 (see Fig. 3b). The mass loading of the PEDOT deposits was found to be 0.08, 0.251 and 0.37 mg/cm^2 for the 5, 15 and 30 minutes of deposition. Areal capacitance was calculated from the slope of discharge curve at each current density. As shown in Fig. 3c, the areal capacitance was found to be 66 mF/cm^2 at a current density of 1 mA/cm^2 for the 30 minute deposited PEDOT. This value was gradually decreased to 47 mF/cm^2 at a current density of 5 mA/cm^2. In the case of 5 minute deposited PEDOT, areal capacitance was varying from 10 to 6 mF/cm^2 at different current density values (see Fig. 3c, Fig. S2, ESI). Similarly, areal capacitance for the 15 minute deposited PEDOT was found to vary from 42 to 30 mF/cm^2. The typical values of gravimetric capacitance were found to be 125, 168 and 175 F/g for the 5, 15 and 30 minutes PEDOT samples. Volumetric capacitance was calculated by dividing the areal capacitance with the corresponding thickness of PEDOT deposited for different times. The variation in the volumetric capacitance at different current densities for the 5, 15 and 30 minute deposited PEDOT samples are shown in Figure 3d. It was observed that the volumetric capacitance was increasing from 125 to 280 F/cm^3 at a current density of 1 mA/cm^2 as the deposition time increased from 5 to 15 minutes. In the case of 30 minute deposited sample, the volumetric capacitance was found to be 300 F/cm^3, indicating that the extended deposition beyond a critical thickness (in this case, 1.5 µm) may not lead to the increase in the volumetric capacitance accordingly. Though there is an enhancement in the areal capacitance of 1.5 times for the 30 minute PEDOT when compared to 15 minute, not much improvement was found in the volumetric and gravimetric capacitances of the two samples. This volumetric capacitance is superior when compared to activated carbon and some of the carbonaceous materials which have been employed as negative electrodes in making asymmetric supercapacitors.[15] Nyquist plots of PEDOT deposited for different times (5-30 min.) are shown in Fig. 3e. The absence of semi-circle in the high frequency regions indicates that negligible charge-transfer resistance across the PEDOT/electrolyte interface. The electrochemical stability of the PEDOT electrode was tested by charging and discharging for 10,000 cycles in the potential of 0.3 to -0.5V. The capacitance is found to be retained up to 87% after 10k cycles as shown in Fig. 3f. Solid state PEDOT symmetric device was made by assembling two PEDOT/Au/PEN electrodes using PVA/H_2SO_4 gel electrolyte (see ESI, Fig. S2). Symmetric solid state PEDOT/Au/PEN//PEDOT/Au/PEN exhibit a volumetric stack capacitance of 20 F/cm^3 at a current density of 0.25 mA/cm^2, in close agreement with the previously reported PEDOT solid state devices on a carbon fiber paper.[49]

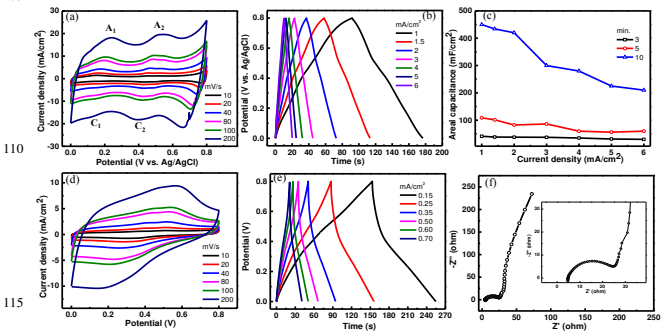

Fig. 4 (a) CV and (b) CD curves of PANI/Au/PEN electrode in 1M H_2SO_4 in 3-electrode configuration. (c) Variation in the areal capacitance with current density for the PANI samples deposited for different times.

View Article Online
DOI: 10.1039/C5TA00829H

(d) CV and (e) CD curves of PANI/Au/PEN//PANI/Au/PEN solid state symmetric supercapacitor using PVA/H_2SO_4 gel electrolyte. (f) Nyqist plot for the PANI solid state device, Inset shows the high frequency portion of the spectrum.

To investigate the electrochemical performance of PANI in the positive potential window (0 to 0.8 V), PANI was electrodeposited on Au/PEN followed by measuring its capacitive behavior in 3-electrode configuration in 1M H_2SO_4 electrolyte. As marked in Fig. 4a, CV scans at different scan rates (10-200 mV/s) exhibit two pairs of redox peaks, A_1/C_1 and A_2/C_2 (see ESI, Fig. S4). The redox pair (A_1/C_1) at lower potential can be attributed to the redox transition of PANI between its leucoemeraldine form (semiconducting) to a polaronicemeraldine form (conducting) while the redox peaks at higher potential can be due to reversible formation of redox pairs such as p-benzo/hydroquinone and p-aminophenol/benzoquinoneimine.[50,51] Due to pseudocapacitve nature of PANI, it exhibits much higher values of capacitance when compared with other conducting polymers. The deviation from the triangular shape of charge-discharge curves is due to Faradaic contribution of PANI in the electrolyte medium (aqueous H_2SO_4), indicating the pseudocapacitive nature of the PANI/Au/PEN electrode as shown in Fig. 4b. The typical mass loadings of the PANI were found to be 0.15, 0.3 and 0.95 mg for the 3, 5 and 10 minutes of deposition. As shown in Fig. 4c, the areal capacitance was increasing gradually from 40 to 110 mF/cm^2 at a current density of 1 mA/cm^2 when deposition time increased from 3 to 5 minutes. This corresponds to the specific mass capacitance of 275 and 362 F/g for the 3 and 5 minutes deposited PANI samples. The maximum areal capacitance was found to be 450 mF/cm^2 (mass specific capacitance of 474 F/g) for the 10 minute deposited PANI at a current density of 1 mA/cm^2. These results are in agreement with the literature reports.[24,25] The volumetric capacitance of 366 F/cm^3 (corresponding areal capacitance of 110 mF/cm^2) was obtained for the 5 minute deposited sample.

Further, two symmetrical PANI/Au/PEN electrodes were glued together with the aid of PVA/H_2SO_4 gel electrolyte, in order to fabricate the solid state symmetric PANI supercapacitor. Cyclic voltammetry and charge-discharge curves for the PANI solid state devices are shown in Figures 4d and 4e. CV scans of the solid state device at different scan rates (10-200 mV/s) exhibit broad redox peaks, due to quasi solid state nature of the gel electrolyte, unlike the liquid H_2SO_4 electrolyte where the distinct redox peaks have been marked (see Fig. 4a). Similarly, the charge-discharge curves were found to be non-linear and the areal cell stack capacitance was found to be 29 mF/cm^2 at a current density of 0.15 mA/cm^2 for the PANI symmetric solid state device (see Fig. 4e). This corresponds to a volumetric stack capacitance of 57 F/cm^3 for the (5 min.) PANI solid state symmetric supercapacitor. The Nyquist plot for the solid state device is shown in Fig. 4f, the vertical nature of the spectrum at low frequency region indicates that the capacitive behavior of the solid state device. In the high frequency region, the spectrum is seen with semi-circle due to charge transfer resistance offered at the electrode/electrolyte interface with a solution resistance of 5 Ω (in this case gel electrolyte).

The representative CVs of PEDOT (30 minute) and PANI (5 minute) in the negative and positive potential windows at a scan rate of 80 mV/s are shown in Fig. 5a. The charge on both the electrodes was matched by balancing the volumetric capacitance of the PEDOT and PANI electrodes. The geometric volume of the electrodes was balanced by the following equation, $V_+/V_- = (C_- \times \Delta E_-)/(C_+ \times \Delta E_+)$ where V_-, V_+, C_-, C_+ and ΔE_-, ΔE_+ are the volume, capacitance and potential windows of the negative and positive electrodes, respectively. Since the overlapping physical area of the positive and negative electrodes is same, the variable parameter is the thickness of the electrodes. The thickness ratio t_+/t_- was found to be 0.51. As obvious, the volume of the electrodes (mostly thickness) was controlled through the electrodeposition time of PEDOT and PANI electrodes. An asymmetric solid state supercapacitor was fabricated by employing optimized thickness of PEDOT and PANI electrodes (see the performance of unoptimised ASC, Fig. S5, ESI). The total thickness of PEDOT (thickness, 4.5 µm) and PANI (thickness, 2.5 µm) was found to be 7 µm in fabricating ASC device. The electrodes were wetted with a thin layer of PVA/H_2SO_4 gel electrolyte followed by assembling the electrodes to form the ASC device. The CVs shown in Fig. 5b were recorded at different scan rates in the potential window of 0-1.6 V (see Fig. S6, ESI). The ASC device exhibits redox behavior due to the redox activity of the conducting polymer electrodes in the electrolyte media. Charge-discharge curves of the ASC device were recorded in the potential window of 0 to 1.6 V at different current densities (0.5-2 mA/cm^2) as shown in Fig. 5c. The curvature in the CD profiles is due to Faradaic contribution from both the conducting polymer electrodes. This ASC device exhibited volumetric stack capacitance of 34 F/cm^3 at a current density of 0.5 mA/cm^2. The cycling stability of the ASC was tested over 10,000 cycles at a current density of 2 mA/cm^2 which showed capacitance retention up to 80% (see ESI, Fig. S6d).[52] The energy and power density of various solid state supercapacitors fabricated in this study are plotted and shown in the Ragone plot in Fig. 5d. The ASC solid state device PANI//PEDOT exhibits highest energy density value of 12 mWh/cm^3 which is superior when compared to the symmetric PEDOT (E = 2 mWh/cm^3) and PANI (E= 5 mWh/cm^3) based solid state supercapacitors.

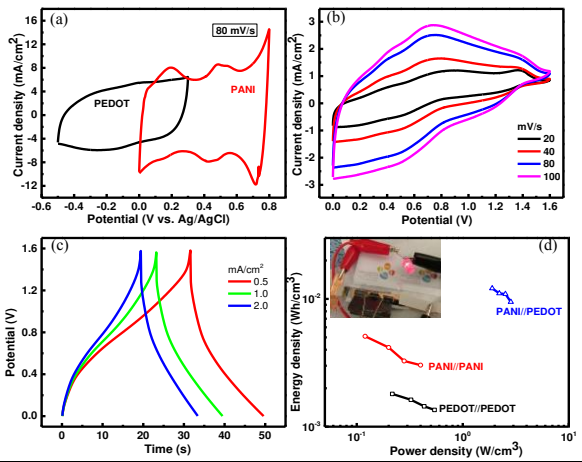

View Article Online
DOI: 10.1039/C5TA00829H

Fig. 5 (a) CV curves of PEDOT/Au/PEN and PANI/Au/PEN electrodes in different potential windows, measured in 1M H_2SO_4 in 3-electrode configuration at scan rate of 80 mV/s. (b) CVs of asymmetric solid state device at different scan rates. (c) Charge-discharge curves of the ASC at different current densities. (d) Ragone plot for the symmetric and asymmetric solid state conducting polymer supercapacitors made in this study, inset shows glowing of an LED using three ASC cells connected in series.

The energy denisty of the solid state ASC is higher by an order of magnitude to that of graphene oxide and onion like carbon supercapacitors (0.8-1 mWh/cm^3) and comparable to that of aqeuous activated carbon based supercapacitors (10 mWh/cm^3) with a power density of 1300 mW/cm^3.[53,54] This solid state ASC device exhibits maximum power density of 2.8 W/cm^3 at an energy density of 9 mWh/cm^3. Further, this ASC PANI//PEDOT exhibits much higher energy density over some of the symmetric supercapacitors based on conducting polymer electrodes such as ppy/paper (E = 1 mWh/cm^3, P = 270 mW/cm^3),[28] and also ASC solid state devices based on MnO_2 Nanowires//Fe_2O_3 Nanotubes (E = 0.55 mWh/cm^3),[22] VO_x//VN (E = 0.61 mWh/cm^3)[55] and H-TiO_2@MnO_2 NWs//H- TiO_2@C core shell NWs (E = 0.3 mWh/cm^3).[56] As the typical mass loading of conducting polymer electrodes was found to be less than 1 mg/cm^2, we have estimated volumetric energy and power denisty of the solid state devices.[57] The higher values of energy denisty for the conducting polymer ASC can be attributed to the redox contribution from both the electrodes which was evident form the electrochemical behavior of the device. The electrochemical activity of the electrode materials in a given electrolyte media and the extent of wettaility decides the performance of the ASC (see ESI, Table S1). Further, three ASC cells were connected in series to demonstrate as a power source in glowing a red light emitting diode (see inset of Fig. 5d).

It is worth-mentioning that Crispin and co-workers have used PEDOT as anode and cathode for fabricating all-polymer based battery with different doping levels.[42,43] Employing same conducting polymer with different doping states come under the category of type III-based devices. As both the electrodes are in the charged state, the open circuit potential can be very high which may deliver high specific energy and power densities. These electrodes have been tested in organic electrolytes rather than aqueous electrolytes. In our case, we relied on two different CPs with complimentary potential windows for the asymmetric design (type II devices). Since PANI shows high electrochemical activity in acid medium (requires protons for redox reactions), we have employed aqueous acid electrolyte for fabricating these conducting polymer based ASC devices.

Recent reports have demonstrated the usage of PANI-porous nanofiber electrodes and PEDOT in designing symmetric and asymmetric supercapacitors by adopting composite materials.[58-60] In contrast to the above studies, we have employed two different CPs as electrode materials in an asymmetric design in order to utilize their complimentary potential windows in extending the working potential window of aqueous based electrolytes beyond 1.23 V which further increses the energy and power density of these ASC devices (E= ½ CV^2 and P = V^2/4R). As the symmetric device based on PEDOT (both anode and cathode) utilize different doping states of the same CP, delivering higher open circuit potential and hence helps in powering an LED bulb by almost 3 minutes.[42] But in our case, the open circuit potentials are small as we use two different CPs in the doped state and we relied on charging it up by applying potential externally which gets harnessed during discharge process in powering an LED. In this case, charge and discharge kinetics are relatively fast er compared to the all-polythiophene rechargeable batteries reported recently.[42] The advantages of our new devices include higher potential window (up to 1.6 V) of aqueous media, faster charge/discharge rates with good cycling stability.

Conclusions

Solid state asymmetric supercapacitors were fabricated by employing the conducting polymers PEDOT and PANI as negative and positive electrode, respectively, and PVA/H_2SO_4 gel electrolyte. The asymmetric devices showed a maximum power density of 2.8 W/cm^3 at an energy density of 9 mWh/cm^3, much higher than other asymmetric solid-state devices based on MnO_2 Nanowires//Fe_2O_3 Nanotubes (E = 0.55 mWh/cm^3), and solid-state devices based on ppy/paper (E = 1 mWh/cm^3) and Pani/pencil/paper (E = 0.32 mWh/cm^3). Tandem configuration of these asymmetric devices was utilised to demonstrate the glowing of a light emiting diode for about 1 minute after charging for 10 seconds.

EXPERIMENTAL SECTION

Materials

Chemicals were used as received without further purification. Analytical grade H_2SO_4 and 3,4-ethylenedioxythiophene (EDOT), aniline (ani) and surface active reagent sodium dodecyl sulphate (SDS, $CH_3(CH_2)_{11}OSO_3Na$) and Polyvinyl alcohol (PVA), were purchased from Sigma-Aldrich.

Electrode preparation and electrochemical deposition

Polyethylene naphthalate (PEN) plastic sheets (thickness, 125 µm) were employed as substrates for making conducting polymer based supercapacitors. These PEN sheets were coated with 150 nm Au/10 nm Ti as conducting layers for electrodepositing conducting polymers. The electrodeposition was performed in a standard three electrode configuration in a glass cell consisting of Au/PEN as working electrode, a platinum wire counter electrode and Ag/AgCl as a reference electrode at room temperature. An electrolyte with 10 mM EDOT + 1 M H_2SO_4 + 10 mM SDS was employed to deposit PEDOT using CHI 660 D Electrochemical Workstation. The role of anionic surfactant is to improve the miscibility of the EDOT monomers in water, and also lowers the oxidation potential below 1V.[30] A constant anodic potential of 0.9 V (vs. Ag/AgCl) was used for different times of 5, 15 and 30 minutes to deposit PEDOT of different thickness over Au/PEN. After the electrochemical deposition, the samples were thoroughly washed with DI water in order to remove the surfactant molecules adsorbed on the surface. Polyaniline (PAni) was electrodeposited using the 0.1 M Aniline + 1M H_2SO_4 as electrolyte by galvanostatic electrodeposition at a constant current density of 0.5 mA/cm^2 for different times.[26]

Material Characterization

View Article Online
DOI: 10.1039/C5TA00829H

Surface morphology and microstructure were imaged by scanning electron microscope (SEM) (Nova Nano 630 instrument, FEI Co., The Netherlands). Energy-dispersive spectroscopy (EDS) analysis was performed with an EDAX Genesis instrument (Mahwah, NJ) attached to the SEM column. Au coating was done by thermal evaporation of 100 nm thick Au on PEN substrate. The film thicknesses were measured using a Veeco Dektak 150 surface profilometer. Raman spectroscopy measurements were carried out on the PEDOT samples using a micro-Raman spectrometer (LabRAM ARAMIS, Horiba-Jobin Yvon). Raman spectra acquired with notch filters cutting at 100 cm^{-1} using a Cobalt laser (473 nm, 5 mW at source) and a laser spot size of 1.5 μm.

Preparation of aqueous gel electrolytes

The electrochemical properties of PEDOT/Au/PEN and PANI/Au/PEN were investigated in both three and two electrode configuration in 1M H_2SO_4 and PVA/H_2SO_4 aqueous gel electrolytes. The PVA/H_2SO_4 gel electrolyte was prepared as follows: 1 g of H_2SO_4 was added into 10 mL of deionized water, followed by adding 1 g of PVA powder. The whole mixture was heated to 85 °C while stirring until the solution became clear.

Fabrication and characterization of asymmetric supercapacitor devices

Solid-state symmetric and asymmetric supercapacitor devices were fabricated by applying the polymer gel electrolyte on the individual negative PEDOT and positive PANI electrodes followed by assembling together and allowed it to dry out the excess water. Cyclic voltammetry (CV), galvanostatic charge−discharge (CD), and electrochemical impedance spectroscopy (EIS) were performed on an electrochemical workstation (model 660D, CH Instruments, Austin, TX, USA). The CVs were tested in different potential windows at varied scan rates, ranging from 10 to 200 mV/s. The CDs were measured at different current densities from 0.1 to 5 mA/cm^2. The EIS was performed in the frequency range from 100 kHz to 0.1 Hz at open circuit potential by applying a small sinusoidal potential of 10 mV signal. All measurements were carried out at room temperature.

Acknowledgement

Research reported in this publication was supported by King Abdullah University of Science and Technology (KAUST). Authors thank the Advanced Nanofabrication, Imaging and Characterization Laboratory at KAUST for their excellent support. Ruiqi Wang wants to thank SRSI for giving this opputinity and also Ms. Tsvetanka B. Sendova for her assitance as a tutor. NK acknowledges the support from SABIC Postdoctoral Fellowship.

Notes and references

Materials Science and Engineering, King Abdullah University of Science and Technology (KAUST), Thuwal 23955-6900

E-mail: husam.alshareef@kaust.edu.sa

† Electronic Supplementary Information (ESI) available:
Fig. S1 (a) CVs of PEDOT in different negative potential windows. (b) Charge-discharge curve for the PEDOT in a wide potential window of 1.4 V.
Fig. S2 (a) and (b) CV and CD of 5 minute deposited PEDOT sample. (c) CV and (d) CD of 15 minute deposited PEDOT sample.
Fig. S3 (a) CV and (b) CDs of symmetric PEDOT/Au/PEN//PEDOT/Au/PEN solid state device using PVA/H_2SO_4 gel electrolyte. (c) Nyquist plot for the symmetric PEDOT solid state device.
Fig. S4 CVs of PANI in different positive potential windows at a scan rate of 80 mV/s. CV is getting narrow down above the potential of 0.8 V.
Fig. S5 Unoptimised CVS of the PANI//PEDOT ASC.
Fig. S6 (a) CVs of ASC device at a scan rate of 80 mV/s in different potential windows. (b) CV scans at a scan rate of 80 mV/s and (c) CDs of ASC device at different current densities after 100 cycles of charging and discharging. (d) Cycling stability of the optimized PANI//PEDOT ASC solid state supercapacitor over 10,000 cycles. Inset shows the charge-discharge curves at a current density of 2 mA/cm^2.
Table S1. Comparison of the electrochemical performance of the ASCs reported in the literature.
See DOI: 10.1039/b000000x/

References

1 M. E. Abdelhamid, A. P. O'Mullane*b* and G. A. Snook, *RSC Adv.*, **2015**, *5*, 11611-11626.
2 L. Nyholm, G. Nyström, A. Mihranyan and M. Strømme, *Adv. Mater.* **2011**, *23*, 3751–3769.
3 C. Meng, C. Liu, L. Chen, C. Hu and S. Fan, *Nano Lett.*, 2010, **10**, 4025-4031.
4 P. Simon and Y. Gogotsi, *Nat. Mater.*, 2008, **7**, 845.
5 M. Winter and R. J. Brodd, *Chem. Rev.,* 2004, **104**, 4245-4270.
6 B. E. Conway, *Electrochemical Supercapacitors, Scientific, Fundamentals and Technological Applications*, Plenum: New York, 1999.
7 G. Wang, L. Zhang and J. Zhang, *Chem. Soc. Rev.,* 2012, **41**, 797-828.
8 Y. Zhai, Y. Dou, D. Zhao, P. F. Fulvio, R. T. Mayes and S. Dai, *Adv Mater.*, 2011, **23**, 4828-4850.
9 Y. Huang, J. Liang and Y. Chen, *Small*, 2012, **8**, 1805-1834.
10 H. Nishihara and T.Kyotani, *Adv. Mater.*, 2012, **24**, 4473-4498.
11 S. L. Candelaria, Y. Shao, W. Zhou, X. Li, J. Xiao, J.-G. Zhang, Y. Wang, J. Liu, J. Li and G. Cao, *Nano Energy*, 2012, **1**, 195-220.
12 J.Jiang, Y. Li, J. Liu, X. Huang, C. Yuan and X. W. Lou, *Adv. Mater.*, 2012, **24**, 5166–5180.
13 M. Zhi, C. Xiang, J. Li, M. Li and N.Wu, *Nanoscale*, 2013, **5**, 72-88.
14 R. Ramya, R. Sivasubramanian, M. V. Sangaranarayanan *Electrochimica Acta*, 2013, **101**, 109–129.
15 F. Wang, S. Xiao, Y. Hou, C. Hu, L. Liu and Y. Wu, *RSC Adv.*, 2013, **3**, 13059-13084.
16 H. C. Gao, F. Xiao, C. B. Ching and H. W. Duan, *ACS Appl. Mater. Interfaces,* 2012, **4**, 7020–7026.
17 D. H. Nagaraju, Q. Wang, P. Beaujuge and H. N. Alshareef, *J. Mater. Chem. A,* 2014, DOI: 10.1039/c4ta03731f.
18 Z. Tang, C. H. Tang and H. Gong, *Adv. Funct. Mater.*, 2012, **22**, 1272–1278.
19 Z. S. Wu, W. C. Ren, D. W. Wang, F. Li, B. L. Liu and H. M. Cheng, *ACS Nano*, 2010, **4**, 5835–5842.
20 C. Yang, J. Shen, C. Wang, H. Fei, H. Bao and G.Wang, *J. Mater. Chem. A*, 2014, **2**, 1458–1464.
21 Y. Hou, L. Chen, P. Liu, J. Kang, T. Fujita and M. Chen, *J. Mater. Chem. A,* 2014, **2**, 10910–10916.
22 P. Yang, Y. Ding, Z. Lin, Z. Chen, Y. Li, P. Qiang, M. Ebrahimi, W. Mai, C. P. Wong and Z. L. Wang, *Nano Lett.*, 2014, **14**, 731−736.
23 Q. T. Qu, Y. S. Zhu, X. W. Gao and Y. Wu, *Adv. Energy Mater.*, 2012, **2**, 950-955.
24 X. Lu, Y. Zeng, M. Yu, T. Zhai, C. Liang, S. Xie ,M.-S. Balogun and Y. Tong, *Adv. Mater.*, 2014, **26**, 3148–3155.

View Article Online
DOI: 10.1039/C5TA00829H

25 T. Zhai, X. Lu, Y. Ling, M. Yu, G. Wang, T. Liu, C. Liang, Y. Tong, and Y. Li, *Adv. Mater.*, 2014, **26**, 5869–5875.
26 K. Wang , H. Wu , Y. Meng and Z. Wei, *Small,* 2014, **10**, 14-31.
27 L. Yuan, X. Xiao, T. Ding, J. Zhong, X. Zhang, Y. Shen, B. Hu, Y. Huang, J. Zhou and Z. L. Wang, *Angew. Chem. Int. Ed.*, 2012, **51**, 4934-4938.
28 L. Yuan, B. Yao, B. Hu, K. Huo, W. Chen and J. Zhou, *Energy Environ. Sci.*, 2013, **6**, 470–476.
29 N. Kurra, J. Park and H. N. Alshareef, *J. Mater. Chem. A,* 2014, **2**, 17058-17065.
30 S. Patra and N. Munichandraiah, *J. Appl. Polym. Sci.*, 2007, **106**, 1160–1171.
31 J. Shen, C. Yang, X. Li and G. Wang, *ACS Appl. Mater. Interfaces,* 2013, **5**, 8467−8476.
32 X. Xiao, T. Ding, L. Yuan, Y. Shen, Q. Zhong, X. Zhang, Y. Cao, B. Hu, T. Zhai, L. Gong et al. *Adv. Energy Mater.*, 2012, **2**, 1328–1332.
33 H. Peng, G. Ma, J. Mu, K. Sun and Z. Lei, *J. Mater. Chem. A*, 2014, **2**, 10384.
34 J. Liu, L. Zhang, H. B. Wu, J. Lin, Z. Shen and X. W. (David) Lou, *Energy Environ. Sci.*, 2014, **7**, 3709.
35 Y. Zhou, H. Xu, N. Lachman, M. Ghaffari, S. Wu, Y. Liu, A. Ugur, K. K. Gleason, B. L. Wardle and Q. M. Zhang, *Nano Energy*, 2014, **9**, 176–185.
36 P. Subramanian, N. Clark, B. Winther-Jensen, D. MacFarlane and L. Spiccia, *Aust. J. Chem.,* 2009, **62**, 133-139.
37 B. Winther-Jensen and K. West, *Macromolecules,* 2004, **37,** 4538-4543.
38 G. Cai, J. Tu, D. Zhou, J. Zhang, Q. Xiong, X. Zhao, X. Wang and C. Gu, *J. Phys. Chem. C,* 2013, **117**, 15967−15975.
39 G. A. Snook and G. Z. Chen, *J. Electroanal. Chem.,* 2008, **612**, 140-146.
40 J. A. Irvin, J. D. Stenger-Smith, In Handbook of Conducting Polymers: Processing and Applications, 3rd ed.; Skotheim, T. A.; Reynolds, J. R., Eds.; CRC Press: Boca Raton, 2007; 9/1;
41 M. Anna, D. Österholm, E. Shen, A. L. Dyer and J. R. Reynolds, *ACS Appl. Mater. Interfaces*, 2013, **5**, 13432−13440.
42 D. Aradilla, F. Estrany, F. Casellas, J. I. Iribarren and C. Alemán, *Org. Electron.*, 2014, **15**, 40-46
43 Y. Xuan, M. Sandberg, M. Berggren and X. Crispin, *Org. Electron.*, 2012, **13**, 632-637.
44 H.-S. Park, S.-J. Ko, J.-S. Park, J. Y. Kim and H.-K. Song, *Sci. Rep.*, 2013, **3**, 976−983.
45 H. J. Ahonen, J. Lukkari, and J. Kankare, *Macromolecules,* 2000, **33**, 6787-6793.
46 X. Chen and O. Inganas, *J. Phys. Chem.*, 1996, **100**, 15202-15206.
47 J. Duay, E. Gillette, R. Liu and S. B. Lee, *Phys. Chem. Chem. Phys.*, 2012, **14**, 3329–3337;
48 L. Bert et al., *Adv. Mater.*, 2003, **15**, 855.
49 B. Anothumakkool, A. Torris, S. N. Bhange, M. V. Badiger and S. Kurungot, *Nanoscale*, 2014, **6**, 5944-5952.
50 D. W. Wang, F. Li, J. P. Zhao, W. C. Ren, Z. G. Chen, J. Tan, Z. S. Wu, I. Gentle, G. Q. Lu and H. M. Cheng, *ACS Nano,* 2009, **3**, 1745 – 1752.
51 D. E. Stilwell and S. M. Park, *J. Electrochem. Soc.*, 1988, **135**, 2254 – 2262.
52 G. A. Snook, G. J. Wilson and A. G. Pandolfo, J. Power Sources, 2009, **186**, 216–223.
53 D. Pech, M. Brunet, H. Durou, P. Huang, V. Mochalin, Y. Gogotsi, P. L.Taberna and P. Simon, *Nat. Nanotechnol.*, 2010, **5**, 651 – 654.
54 W. Gao, N. Singh, L. Song, Z. Liu, A. L. M. Reddy, L. Ci, R. Vajtai, Q. Zhang, B. Wei and P. M. Ajayan, *Nat. Nanotechnol.*, 2011, **6**, 496 – 500.
55 X. Lu, M. Yu, T. Zhai, G. Wang, S. Xie, T. Liu, C. Liang, Y. Tong and Y. Li, *Nano Lett.*, 2013, **13**, 2628-2633.
56 X. Lu, M. Yu, G. Wang, T. Zhai, S. Xie, Y. Ling, Y. Tong, Y. Li, *Adv. Mater.,* 2013, **25**, 267.
57 M. D. Stoller and R. S. Ruoff, *Energy Environ. Sci.*, 2010, **3**, 1294–1301.
58 M. Dirican, M. Yanilmaza and X. Zhang, *RSC Adv.,* 2014, **4**, 59427-59435.
59 D. Aradilla, D. Azambuja, F. Estrany, M. T. Casas, C. A. Ferreirae and C. Alemán, *J. Mater. Chem.*, 2012, **22**, 13110- 13122.
60 L. Fan, N. Zhang and K. Sun, *Chem. Commun.*, 2014, **50**, 6789-6792.